Vehicle Chassis Decoupling Control Based on Neural Network Inverse Method

Jun Yang[1.] Linfeng Zhao[2.] Wuwei Chen[3.] He Huang[4.] Guang Xia[5.]

School of Mechanical and Automotive Engineering, Hefei University of Technology, Hefei 230009 China

ABSTRACT

In order to eliminate the interference and coupling among automobile chassis electronic control subsystems, an integrated decoupling control approach based on neural network inverse method was proposed. The integration of active front steering (AFS), direct yaw moment control (DYC) and active suspension (ASS) was studied. According to Inter-actor algorithm, the reversibility of chassis system was analyzed and a BP neural network inverse system of the multivariable chassis system was obtained. Designing a close-loop controller and combining it with neural network inverse system, a compound controller was completed to improve dynamic performance. The simulation results showed that the proposed decoupling control approach could eliminate the interference and couple among automobile chassis electronic control subsystems, and improve the automobile handling and stability performance.

Keywords: Chassis, Decoupling control, Neural network, Inverse method I-INCE Classification of Subjects Number(s): 13.2.1

1. INTRODUCTION

In recent years, to make up a use limited range control lack for single control system, it becomes a research spot in vehicle dynamics for integrated control of vehicle chassis every subsystem to discover functional potential. Due to aiming at some partial function in chassis every electronic control subsystem, it will inevitable appear coupling and interference among the subsystems for designing chassis integrated control system. If we decouple to chassis integrated system of inter-coupling for each channel when designing the control system, it will simplified complex chassis integrated control system design. A vast variety of research results can be found in the literature[1]~[4]. In this paper, we present an control method based on neural network inverse [5] to decouple among AFS, DYC and ASS systems.

2. Model of control system

A vehicle model included lateral, yawing and rolling DOF is shown in Fig.1. Where u_c, β, r, ϕ are the longitudinal speed, side-slip angle, yaw rate and roll angle; m, m_s, m_f, m_r are mass of vehicle, suspension, front unsprung and rear unsprung; a, b are front , rear wheelbase; I_z, I_x are moment of inertia of yawing and rolling; I_{xz} is a product of inertia of yawing and rolling movement; k_F, k_R are cornering

[1]yangjun8510@hotmail.com
[2]zhao.lin.feng@163.com
[3]hfgdcjs@126.com
[4]cranehh@qq.com
[5]xiaguang008@163.com

stiffness of front and rear wheels; δ_f, δ_c, T_z, T_ϕ are respectively the front wheel angle exerted by driver, the front wheel angle compensation, yawing control moment, suspension rolling moment; K_ϕ, D_ϕ are coefficients of stiffness and damping of suspension rolling.

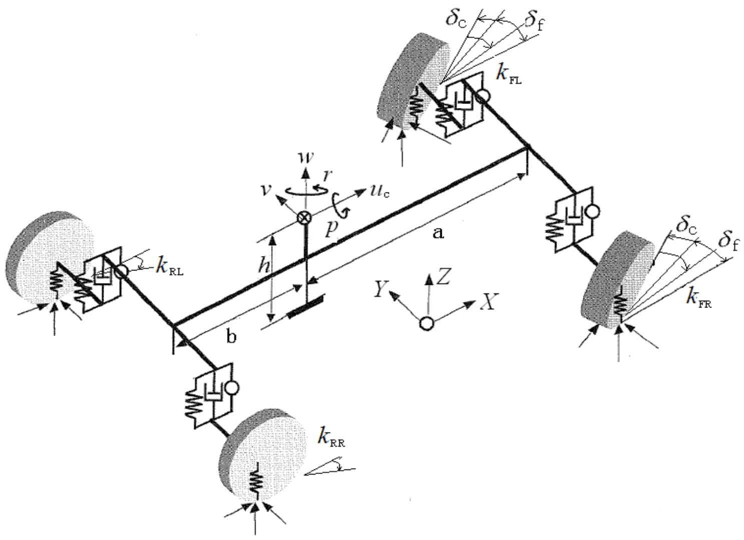

Fig.1 Vehicle model

If we define the state vector as $\boldsymbol{x}=(\beta \quad r \quad \phi \quad \dot{\phi})^{\mathrm{T}}$, control input vector as $\boldsymbol{u}=(\delta_c \quad T_z \quad T_\phi)^{\mathrm{T}}$, system output vector as $\boldsymbol{y}=(\beta \quad r \quad \phi)^{\mathrm{T}}$, then the state-space equation of this integrated system can be written as following:

$$\begin{cases} \boldsymbol{M}\dot{\boldsymbol{x}} = \boldsymbol{K}\boldsymbol{x} + \boldsymbol{N}\boldsymbol{u} + \boldsymbol{Q}\delta_{\mathrm{F}} \\ \boldsymbol{y} = \boldsymbol{C}\boldsymbol{x} \end{cases} \tag{1}$$

where

$$\boldsymbol{M} = \begin{pmatrix} mu_{\mathrm{c}} & am_{\mathrm{f}} - bm_{\mathrm{r}} & 0 & m_{\mathrm{s}}h \\ (am_{\mathrm{f}} - bm_{\mathrm{r}})u_{\mathrm{c}} & I_{\mathrm{z}} & 0 & I_{\mathrm{xz}} \\ 0 & 0 & 1 & 0 \\ m_{\mathrm{s}}hu_{\mathrm{c}} & I_{\mathrm{xz}} & 0 & I_{\mathrm{x}} \end{pmatrix}$$

$$\boldsymbol{K} = \begin{pmatrix} -2(k_{\mathrm{F}} + k_{\mathrm{R}}) & -mu_{\mathrm{c}} + \dfrac{2(bk_{\mathrm{R}} - ak_{\mathrm{F}})}{u_{\mathrm{c}}} & 0 & 0 \\ 2(bk_{\mathrm{R}} - ak_{\mathrm{F}}) & (bm_{\mathrm{r}} - am_{\mathrm{f}})u_{\mathrm{c}} - 2\dfrac{a^2k_{\mathrm{F}} + b^2k_{\mathrm{R}}}{u_{\mathrm{c}}} & 0 & 0 \\ 0 & 0 & 0 & 1 \\ 0 & m_{\mathrm{s}}hu_{\mathrm{c}} & m_{\mathrm{s}}gh - K_\phi & -D_\phi \end{pmatrix}$$

$$\boldsymbol{N} = \begin{pmatrix} 2k_{\mathrm{F}} & 0 & 0 \\ 2k_{\mathrm{F}} & 1 & 0 \\ 0 & 0 & 0 \\ 0 & 0 & 1 \end{pmatrix}, \boldsymbol{Q} = \begin{pmatrix} 2k_{\mathrm{F}} \\ 2ak_{\mathrm{F}} \\ 0 \\ 0 \end{pmatrix}, \boldsymbol{C} = \begin{pmatrix} 1 & 0 & 0 & 0 \\ 0 & 1 & 0 & 0 \\ 0 & 0 & 1 & 0 \end{pmatrix}$$

It is quite obvious that Eq. (1) is a typical multi-variable systems of three inputs, output. Due to the connection of longitudinal, lateral and vertical force of tires, and then body rolling, pitching influence each other with longitudinal and lateral movement, makes the systems of AFS, DYC and ASS existing a strong coupling relationship. In order to simply the design of the integrated system of AFS/DYC/ASS, need to decouple the multi-variable integrated system of the above three control circuit shown in Eq. (1).

3. Design decoupling control system based on neural network inverse method reversibility analysis of system

We can prove reversibility of state equation of multi-input and multi-output chassis integrated system with Interactor algorithm which is shown in Eq. (1): to calculate the each derivative of time of output vector $\boldsymbol{y}$ till containing input vector $\boldsymbol{u}$ in output of the derivative equation, which are summarized as in Eq. (1) below.

$$\begin{aligned} \dot{y}_1 = \dot{\beta} = & -2(k_{\mathrm{F}} + k_{\mathrm{R}})\beta / mu_c + 2r(bk_{\mathrm{R}} - ak_{\mathrm{F}}) / mu_c^2 \\ & - m_s h\ddot{\phi} / mu_{\mathrm{c}} - (am_{\mathrm{f}} - bm_{\mathrm{r}})\dot{r} / mu_{\mathrm{c}} - r + 2k_{\mathrm{F}}(\delta_f + \delta_{\mathrm{c}}) / mu_{\mathrm{c}} \end{aligned} \tag{2}$$

If we assume $\boldsymbol{Y}_1 = \dot{y}_1$, the rank of Jacobian matrix of input vector $\boldsymbol{u}$ shows as following

$$t_1 = rank\left[\frac{\partial \boldsymbol{Y}_1}{\partial u^{\mathrm{T}}}\right] = rank\left[\begin{matrix} \frac{\partial \dot{y}_1}{\partial \delta_{\mathrm{c}}} & \frac{\partial \dot{y}_1}{\partial T_{\mathrm{z}}} & \frac{\partial \dot{y}_1}{\partial T_{\phi}} \end{matrix}\right] = 1 \tag{3}$$

$$\begin{aligned} \dot{y}_2 = \dot{r} = & \, 2(bk_{\mathrm{R}} - ak_{\mathrm{F}})\beta / I_{\mathrm{z}} - 2(a^2 k_{\mathrm{F}} + b^2 k_{\mathrm{R}}) r / I_{\mathrm{z}} u_{\mathrm{c}} \\ & - I_{\mathrm{xz}}\ddot{\phi} / I_{\mathrm{z}} - (am_{\mathrm{f}} - bm_{\mathrm{r}})(\dot{\beta} + r)u_{\mathrm{c}} / I_{\mathrm{z}} + T_{\mathrm{z}} / I_{\mathrm{z}} + 2ak_{\mathrm{F}}(\delta_f + \delta_{\mathrm{c}}) / I_{\mathrm{z}} \end{aligned} \tag{4}$$

If we assume $\boldsymbol{Y}_2 = [\dot{y}_1 \quad \dot{y}_2]^{\mathrm{T}}$, the rank of Jacobian matrix of input vector $\boldsymbol{u}$ shows as following

$$t_2 = rank\left[\frac{\partial \boldsymbol{Y}_2}{\partial u^{\mathrm{T}}}\right] = rank\begin{bmatrix} \frac{\partial \dot{y}_1}{\partial \delta_{\mathrm{c}}} & \frac{\partial \dot{y}_1}{\partial T_{\mathrm{z}}} & \frac{\partial \dot{y}_1}{\partial T_{\phi}} \\ \frac{\partial \dot{y}_2}{\partial \delta_{\mathrm{c}}} & \frac{\partial \dot{y}_2}{\partial T_{\mathrm{z}}} & \frac{\partial \dot{y}_2}{\partial T_{\phi}} \end{bmatrix} = 2 \tag{5}$$

$$\begin{aligned} & \dot{y}_3 = \dot{\phi} \\ & \ddot{y}_3 = \ddot{\phi} = -D_{\phi}\dot{\phi} / I_{\mathrm{x}} - (K_{\phi} - m_{\mathrm{s}} gh)\phi / I_{\mathrm{x}} - I_{\mathrm{xz}}\dot{r} / I_{\mathrm{x}} - m_{\mathrm{s}} h(\dot{\beta} + r)u_{\mathrm{c}} / I_{\mathrm{x}} + T_{\phi} / I_{\mathrm{x}} \end{aligned} \tag{6}$$

If we assume $\boldsymbol{Y}_3 = [\dot{y}_1 \quad \dot{y}_2 \quad \ddot{y}_3]^{\mathrm{T}}$, the rank of Jacobian matrix of input vector $\boldsymbol{u}$ show as following

$$t_3 = rank\left[\frac{\partial \boldsymbol{Y}_3}{\partial u^{\mathrm{T}}}\right] = rank\begin{bmatrix} \frac{\partial \dot{y}_1}{\partial \delta_{\mathrm{c}}} & \frac{\partial \dot{y}_1}{\partial T_{\mathrm{z}}} & \frac{\partial \dot{y}_1}{\partial T_{\phi}} \\ \frac{\partial \dot{y}_2}{\partial \delta_{\mathrm{c}}} & \frac{\partial \dot{y}_2}{\partial T_{\mathrm{z}}} & \frac{\partial \dot{y}_2}{\partial T_{\phi}} \\ \frac{\partial \ddot{y}_3}{\partial \delta_{\mathrm{c}}} & \frac{\partial \ddot{y}_3}{\partial T_{\mathrm{z}}} & \frac{\partial \ddot{y}_3}{\partial T_{\phi}} \end{bmatrix} = 3 \tag{7}$$

Due to existing non-negative integer $R_1 = 1$, $R_2 = 1$, $R_3 = 2$, makes t_3 to equal output numbers of system shown in Eq. (1), then vector relative order of system is $R = [R_1 \quad R_2 \quad R_3]^{\mathrm{T}} = [1 \quad 1 \quad 2]^{\mathrm{T}}$, and $\sum_{i=1}^{3} R_i = n = 4$ (n is system order). As we known from the implicit function theorem, it will be exist inverse system of Eq. (1), and the output $\boldsymbol{u}$ of inverse system (input of original system) can be written as

$$\boldsymbol{u} = \varphi(\boldsymbol{x}, \dot{y}_1, \dot{y}_2, \ddot{y}_3) = \varphi(\boldsymbol{x}, \boldsymbol{v}) \tag{8}$$

Where $\boldsymbol{v} = [v_1 \quad v_2 \quad v_3]^{\mathrm{T}} = [\dot{y}_1 \quad \dot{y}_2 \quad \ddot{y}_3]^{\mathrm{T}}$, $\varphi(\bullet)$ is the non-linear relationship of output and input of inverse system. If we can regard $z_1 = y_1$, $z_2 = y_2$, $z_{31} = y_3$, $z_{32} = \dot{z}_{31} = \dot{y}_3$, $v_1 = \dot{y}_1$, $v_2 = \dot{y}_2$, $v_3 = \ddot{y}_3$ as the input of inverse system, then standard inverse system of Eq. (1) can be written as

$$\begin{cases} \dot{z}_1 = v_1 \\ \dot{z}_2 = v_2 \\ \dot{z}_{31} = z_{32} \\ \dot{z}_{32} = v_3 \\ \boldsymbol{u} = \bar{\varphi}\left(z_1 \quad z_2 \quad z_{31} \quad z_{32} \quad v_1 \quad v_2 \quad v_3\right) \end{cases} \tag{9}$$

As can be seen from Eq. (9), the pseudo linear system composed with putting inverse system to cascade before original system, will be equal to two first order and one second order integral linear subsystems, so we can treat control problem of strong coupling multivariable system included AFS, DYC and ASS as controlling two first order and one second order integral linear subsystems shown in Fig. 2.

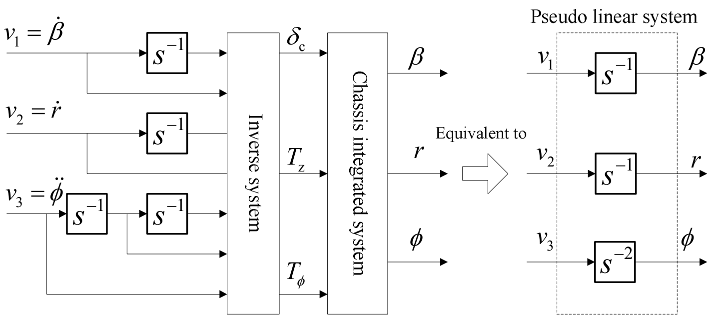

Fig. 2 Configuration of the pseudo-linear system

Neural network inverse system configuration and Training

The analytical inverse system expression of chassis integrated system based on accurate mathematical model of Eq. (9) represents the decoupling characteristics of the pseudo-linear system only if the original system parameter is accurate, available and constant. To improve the self-adaptivity to the parameter variation and the robustness with respect to load perturbation, the static neural network and integral is applied to construct the inverse system of Eq. (9).

From Eq. (9) it can be known that the input level includes β, r, ϕ, $\dot{\phi}$, $\dot{\beta}$, $\dot{r}$ and $\ddot{\phi}$, and output level includes δ_c, T_z and T_ϕ. Therefore the amount of neurons on the input level is set to be 7, and it is 3 for the output level. The number of neurons on the implicit level is determined to be 15 by trail and error. The nonlinear mapping of the reverse system is approached by using static neural network. 4 integrals are used to represent the dynamic characteristics of the reverse system. Therefore the obtained neural network reverse system structure of chassis integrated system is Fig.3, shown as Fig.4. Tansig is used as transfer function for the input level and implicit level of BP network, while purelin is used for output level.

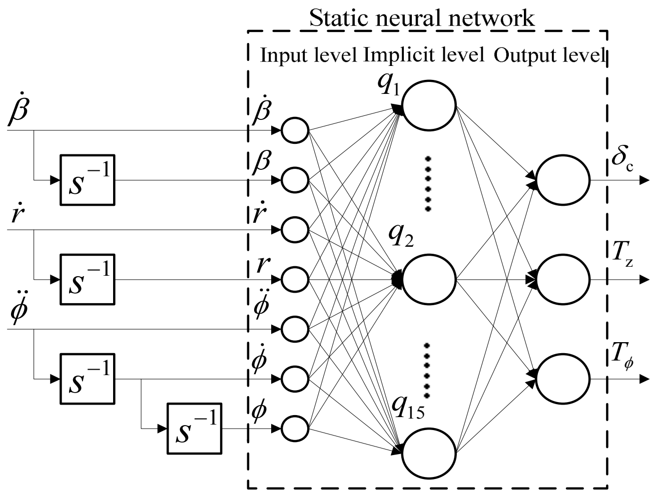

Fig. 3 Configuration of inverse system BP neural network

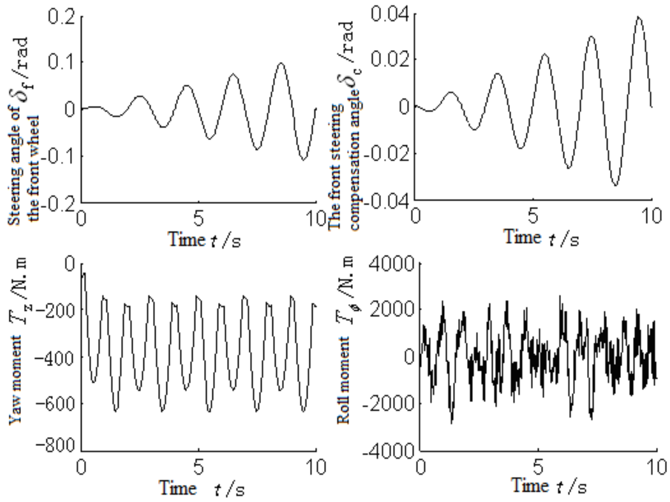

Fig. 4 The stimulating signal of neural network reverse system for training

It is set that the vehicle speed to be 100km/h, the driver's input front steering to sinusoidal curve with varying amplitude, the front steering compensation angle to be δ_c, yaw moment T_z, and the stimulation input signal for suspension roll moment T_ϕ are shown in Fig. 4.

The responses of yaw rate r, side-slip angle β and roll angle ϕ are sampled with 5ms period. According to the five point numerical differential method $\dot{r}$, $\dot{\beta}$, $\dot{\phi}$ and $\ddot{\phi}$ as the first order and second order numerical differentials of r, β and ϕ are calculated. By recombination of the data above, 2000 sets of training data sets [β, $\dot{\beta}$, r, $\dot{r}$, ϕ, $\dot{\phi}$, $\ddot{\phi}$]and [δ_c, T_z, T_ϕ] are obtained. The premnmx function of the neural network tool box in Matlab is used to normalize the network input/output data. In network simulation test, the new data are preprocessed by tramnmx in the same way, and finally normalized by postmnmx. BP neural network is established by newff, and trainlm of Levenberg-Marquardt algorithm is selected as training function. The established BP network is trained by train function, with 500 training times, 0.05 learning efficiency, 10^{-3} network target error. The required training accuracy is achieved by 72 times training.

Design PD controller

The integrated system transfer three single input and output systems which is non-interference after the system decoupling, like as first order AFS subsystem, first order DYC subsystem and second order ASS subsystem. In order to improve the quality of response of integrated system, we design PD controller and joint controller composed with neural inverse system for effective control shown in Fig. 5.

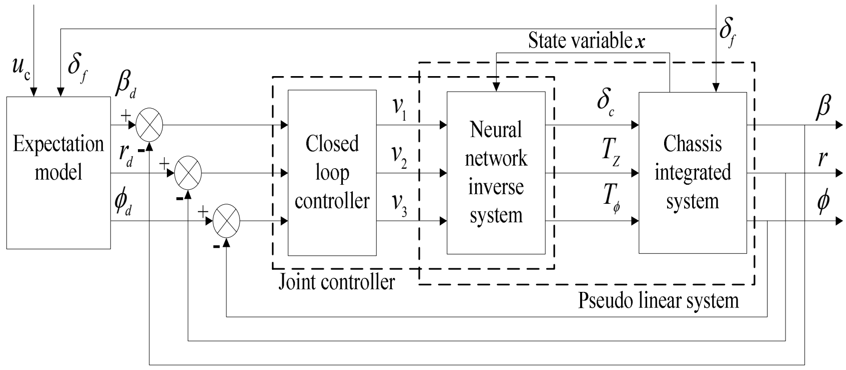

Fig. 5 Configuration of chassis integrated system

The pseudo linear system gotten by decoupling has one to one relationship between output and input of system, so using the methods of PID control, pole placement or quadratic optimal control and so on for the linear system theory of single variable design the controller. Therefore, we design the PD closed loop controller as following based on decoupling system.

$$\boldsymbol{v} = \boldsymbol{K}_{\mathrm{P}}\mathrm{diag}\{\boldsymbol{e}\} + \boldsymbol{K}_{\mathrm{d}}\mathrm{diag}\{\boldsymbol{de}\} \tag{10}$$

Where $\boldsymbol{e}$, $\boldsymbol{de}$ are the deviation and deviation rate of system output signal respectively; $\boldsymbol{K}_{\mathrm{p}}$, $\boldsymbol{K}_{\mathrm{d}}$ are the coefficients of proportion and differential.

As we are shown in Fig. 5, the expectation model of vehicle generates the reference value of dynamic response according to driver input, then getting the expected value of side-slip angle and yaw rate .

$$\begin{cases} \beta_{\mathrm{d}} = \dfrac{\dfrac{2k_{\mathrm{F}}(2a^2k_{\mathrm{F}} + 2b^2k_{\mathrm{R}})}{2ak_{\mathrm{F}} - 2bk_{\mathrm{R}} + mu_c^2} - 2bk_{\mathrm{F}}}{\dfrac{(2k_{\mathrm{F}} + 2k_{\mathrm{R}})(2a^2k_{\mathrm{F}} + 2b^2k_{\mathrm{R}})}{2ak_{\mathrm{F}} - 2bk_{\mathrm{R}} + mu_c^2} + 2bk_{\mathrm{R}} - 2ak_{\mathrm{F}}}\delta_f \\ r_{\mathrm{d}} = \min\left\{\left|\dfrac{u_{\mathrm{c}}\delta_f}{(a+b)(1+Ku_c^2)}\right|, \left|\dfrac{\mu g}{u_{\mathrm{c}}}\right|\mathrm{sgn}(\delta_f)\right\} \end{cases} \tag{11}$$

Where, μ is a tire-road friction coefficient; K is a under-steer coefficient.

4. Simulation calculation and Results analysis

In this section, simulation evaluations are carried out to verify the performance of the proposed method discussed above. We set PD closed loop controller coefficients as Kp=diag{18 52 5000}, Kd= diag {4.5 3 10} according to repeated adjustment。 Set the initial state speed as u_{c}=80 km/h, tire-road friction coefficient as $\mu = 0.85$, rolling stiffness coefficient of suspension as K_ϕ =65590 N.m.rad^{-1}, rolling damping coefficient of suspension as D_{ϕ} =2100N.m.rad^{-1}.s.

Two typical road conditions are selected, first of which is the road whose maximum coefficient μ is 0.8 and second of which is the ice road with maximum μ around 0.2. The simulation results for the left front tire can be seen in Fig.6 and Fig.7 below.

The common PD control, AFS/DYC/ASS joint control (three sub-controllers control independent at the same time) and decoupled PD control based neural network inverse system can be used to simulate in two typical road conditions, and then comparative analysis between simulated and expected value.

Single line change simulation

According to GB/T6323.1-94, a single line change simulation is carried out with driver's front wheel steering angle amplitude 0.08rad, frequency 0.5Hz, the obtained response curves of yaw rate, side-slip angle and roll angle is shown in Fig. 6. In Figure (a), compared with coordinated control, simple PD control and decoupled PD control both achieve better yaw rate tracking effect, but the overshoot of decoupled PD control is relatively smaller. In Figure (b), the side-slip angle controlled by decoupled PD controller is suppressed within a smaller range, and therefore the vehicle handling stability is improved. In Fig (c), because one output is completed controlled by one input due to the decoupled PD controller, the vehicle stability under extreme condition is improved.

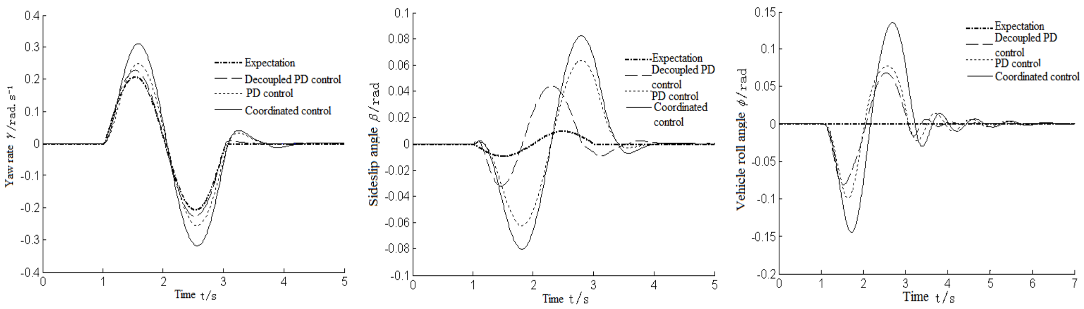

(a) Yaw rate (b) side-slip angle (c) Roll angle

Fig. 6 Single line change simulation

Under single line change condition, the peak values of yaw rate, side-slip angle and roll angle with different control method applied is shown in Table 1. Compared with simple PD control and coordinated control, with decoupled PD control applied, the yaw rate peak value decreases 12% and 29% respectively, the side-slip angle peak value decreases 33.9% and 49.4%, and the roll angle peak value decreases 21.9% and 49%.

Table1- Comparison of peak value of single line change simulation result

Control Method	Yaw rate r/rad.s^{-1}	Side-slip angle β/rad	Roll angle ϕ/rad
Expectation	0.2	0.01	0
Decoupled PD control	0.22	0.041	0.075
PD control	0.25	0.062	0.096
Joint control	0.31	0.081	0.147

Step steering simulation

According to GB/T6323.2-94, the driver's step steering angle amplitude input is set to be $\frac{\pi}{2}$, the the comparison of obtained yaw rate, side-slip angle and roll angle is shown as Fig. 7.

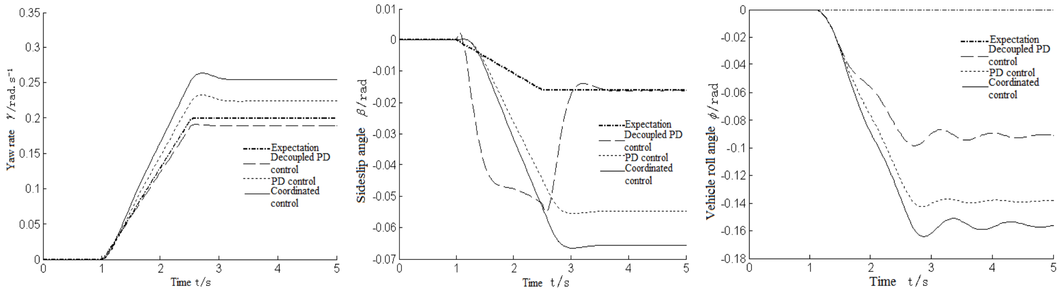

(a) Yaw rate (b) Side-slip angle (c) Roll angle

Fig. 7 Step steering simulation

It is obvious that under step steering condition, the vehicle yaw rate approaches the expected value with decoupled PD control, and the side-slip angle and roll angle is within a controllable range. With the coordinated control applied on chassis, because each subsystem aims at local performance, the amplitudes of yaw rate, side-slip angle and roll angle are large. Because the simple PD control fails to take the control loop coupling effect into consideration, it is inevitable to negatively influence other target with one single target aimed. The resultant yaw rate, side-slip angle and roll angle deviate from the expectations. The yaw rate, side-slip angle and roll angle peak values with different control methods applied is shown as Table 2. Compared with simple PD control and coordinated control, with decoupled PD control, the vehicle yaw rate peak value decreases 19.1% and 26.4%, the side-slip angle peak value drops 1.8% and 16.7%, and the roll angle peak value drops 32.4% and 41.5%.

Table 2- Comparison of step steering simulation result peak values

Control Method	Yaw Rate r/rad.s^{-1}	Side-slip Angle β/rad	Roll Angle ϕ/rad
Expected Value	0.2	0.017	0
Decoupled PD Control	0.195	0.055	0.096
PD Control	0.241	0.056	0.142
Coordinated Control	0.265	0.066	0.164

5. CONCLUSIONS

We have developed a control method for the chassis integrated system. Neural network inverse control method of multivariable chassis system is applied in designing vehicle chassis decoupling control system, the reversibility of chassis system was analyzed and a BP neural network inverse system of the multivariable chassis system was obtained. The pseudo linear system gotten by decoupling has one to one relationship between output and input of system, the every control circuit decouples each other. The proposed methods were shown through simulations to be very promising compared with those other control. Moreover, the chassis integrated control based on neural network inverse system significantly realizes the favorable vehicle state tracking and stability, which has a certain robustness.

ACKNOWLEDGEMENTS

This paper is supported by National Natural Science Foundation of China (Grant No. 51075112, Grant No. 51175135, Grant No. 51375131) and Natural Science Foundation of Anhui Province of China (Grant No. 2013AKZR0077).

REFERENCES

1. Trachtler A. Integrated vehicle dynamics control using active brake, steering and suspension system [J]. International Journal of Vehicle Design, 2004, Vol. 36 (1), pp. 1-12.
2. Karbalaei R, Ghaffari A, Kazemi R, et al. A new intelligent strategy to integrated control of AFS/DYC based on fuzzy logic [J]. International Journal of Mathematical, Physical and Engineering Sciences, 2007, Vol. 33 (6), pp. 47-52.
3. Chen Wuwei, Xu Juan, Hu Fang, et al. I/O decoupling and decoupling proportion and differential control of nonlinear full car system [J]. Chinese Journal of Mechanical Engineering, 2007, Vol. 43 (2), pp. 64-70.
4. Kazuyu Kitajima, Huei Peng. H_∞ control for integrated side-slip, roll and yaw controls for ground vehicles [C]. Proceedings of AVEC 2000, 5th International Symposium on Advanced Vehicle Control, Michigan, 2000: 22-24.
5. Duo Zhang, Guohai Liu, Longsheng Wang, et al. Active safety neural network inverse decoupling control for multi-wheel independently driven electric vehicles [C]. 2013 Vehicle Power and Propulsion Conference. pp. 1-4.
6. Zhang Jinzhu, Zhang Hongtian. Vehicle stability control based on adaptive PID control with single neuron network [C]. 2010 2nd International Asia Conference on Informatics in Control, Automation and Robotics (CAR), Wuhan, 2010, Vol. 1, PP. 434-437.